# ANOMALY DETECTION AND DIAGNOSTICS OF A WHEEL LOADER USING DYNAMIC MATHEMATICAL MODEL AND JOINT PROBABILITY DISTRIBUTIONS

PhD Tomi Krogerus, PhD Mika Hyvönen, MSc Joni Backas, Professor Kalevi Huhtala
Tampere University of Technology
Department of Intelligent Hydraulics and Automation
P.O.Box 589
33101 Tampere, Finland
E-mail: tomi.krogerus@tut.fi

## ABSTRACT

In this paper, we present anomaly detection and diagnostics for articulated frame steered hydraulic wheel loader. The presented methodology is based on the analysis and comparison of the responses of a dynamic mathematical model and a real wheel loader using a joint probability distribution of correlation coefficients of multiple variables. The behaviour of an undamaged machine is modelled by probability density functions of the correlation coefficients using histograms and test how well the future behaviour fits the model. First, the time series data of multiple variables are segmented into segments of the same length. Correlation coefficients are then calculated for each segment and the distributions of the correlation coefficients are estimated by computing probability density functions using histograms. Finally, the joint probabilities that the correlations in the data segments of the time series data are observed are calculated using the already computed histograms. The diagnostics is based on the combination of static threshold and threshold based on mean value of joint probabilities. The dynamic mathematical model of the wheel loader is presented with verification results. A jammed flushing valve of the hydrostatic transmission was used as an anomaly to study the changes in the joint probability values. Finally, the efficiency of the presented method is presented with good results regarding detection of anomalies and diagnostics of the wheel loader.

KEYWORDS:     Diagnostics, time series, anomaly detection, joint probability, correlation coefficients, simulation, dynamic mathematical model, wheel loader, hydraulics

## 1. INTRODUCTION

Diagnostics and fault detection of machine systems have been studied widely and significant amount of literature exist of it. See for example the following surveys [1], [2], [3]. Diagnostic techniques can be generally classified into two approaches, depending on whether the diagnostics assessment is based on deterministic or on stochastic information (e.g. historical, statistical parameters) [4], [5]. Segmentation and feature extraction are two major components of time series analysis employed in diagnostics. Segmentation [6], [7] is a method which allows the dividing of time series data into smaller groups of data sets which describe the patterns of the measured variables. Feature extraction involves extracting relevant and discriminating information, and in so doing, reducing data dimensionality: see [8], [9]. The extracted features

are then used to derive the status and the condition of the system using for example classification methods [9], [10], [11].

The use of simulation models in the development of highly automated machines is becoming a necessity [12], [13], [14]. Models are typically created during the early development phase of a machine. However, these simulation models are not effectively utilized in the later phases of product lifecycle. In this paper, previously developed methodology [15], [16], originally developed in simulator environment [14], for using a dynamic simulation model of the machine system for diagnostics purposes is used and the results are verified in real machine environment. In this methodology, the responses of a real undamaged machine and a dynamic mathematical model of this machine are analysed and compared from a stochastic point of view based on probabilities. This means, a statistical model using certain drive sequences of a real undamaged (i.e. healthy) machine and simulated undamaged machine is build and tested how well the future behaviour fits this model.

In the following sections, we present an approach to the anomaly detection and diagnostics of a wheel loader. Section 2 introduces our studied machine, a wheel loader and its dynamic mathematical model. Section 3 describes the methodology to analyse time series data. In section 4 experiments to acquire the data and analysis results are presented, followed by the conclusion in section 5.

## 2. STUDIED WHEEL LOADER AND DYNAMIC MATHEMETICAL MODEL

In this chapter, the studied wheel loader and the developed dynamic mathematical model are presented with verification results. The wheel loader was engineered at the Department of Intelligent Hydraulics and Automation at Tampere University of Technology [17]. The wheel loader is shown in Fig. 1.



Figure 1. Studied wheel loader [17].

### 2.1. Analysed sub-system – hydrostatic drive (HSD)

An overview of the hydraulic systems of the wheel loader, which are related to the analysis performed in this study, is given here. To be precise, the analysed sub-system is hydrostatic drive (HSD). More details about the machine are presented in [17]. Fig. 2 shows a simplified hydraulic circuit of the closed loop HSD of the machine.
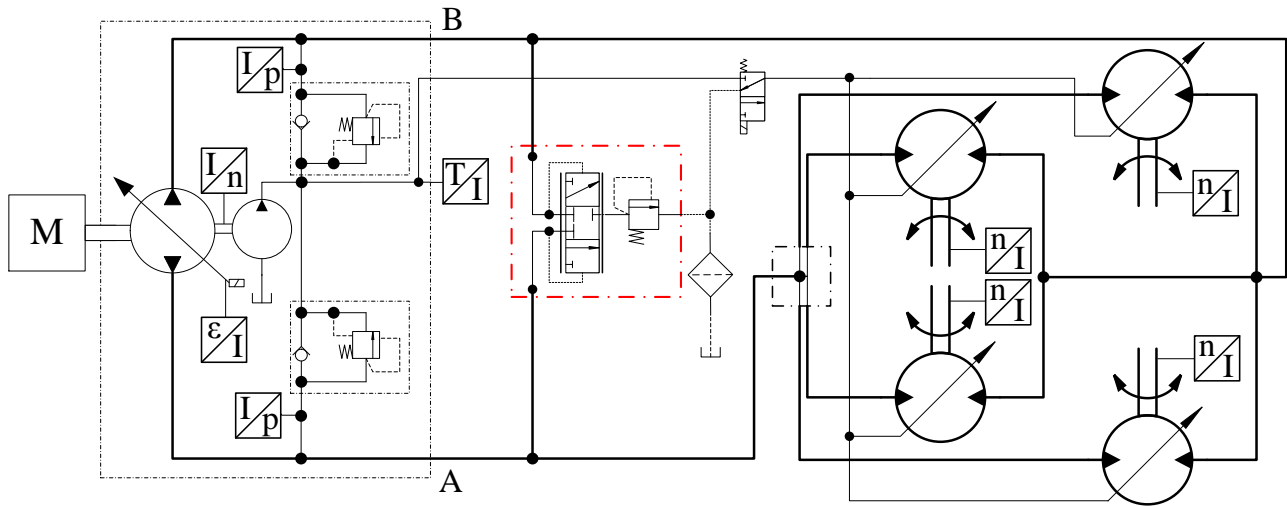
*Figure 2. HSD of studied wheel loader. Flushing valve is highlighted with coloured dash line.*

The main source of power is a 100 kW four-cylinder diesel engine. The HSD pump has a displacement of 110 $cm^3$/r and contains various integrated hydraulic components, sensors and electronics to implement the closed-loop control of the swivel angle and the data communication.

Both the diesel engine and the pump are connected to the control system of the machine via the CAN bus. They also have separate control units, which are connected to the CAN bus, offering data from integrated sensors. Therefore, via the CAN bus several parameters related to the operation of these components, e.g. rotational speed of the diesel engine and displacement of the HSD pump, can be monitored and recorded for later analysis.

Every wheel of the machine is equipped with a slow speed hydraulic hub motor, with a displacement of 470 $cm^3$/r. The displacement of the motors can also be reduced into 235 $cm^3$/r when the displacement is bisected. Each motor has a pressure controlled holding brake and an integrated sensor for measuring rotational speed. A separate hydraulic gear pump provides the power needed by the steering system. The steering of the machine can be controlled using proportional flow control valve and two symmetrically placed hydraulic cylinders.

The valve connected to the ports A and B of the pump is called a flushing valve. A certain amount of flow is always circulated through this valve to the tank from the lower pressure side of the pump. This reduces the temperature of the fluid and the amount of impurities in it. In this research, this valve has been taken out to simulate a jammed flushing valve of the hydrostatic drive transmission which is used as an anomaly to study the changes in the joint probability values and to verify the results of anomaly detection and diagnostics. This component was selected because jamming of the valve cannot be directly recognized by the operator during normal use of the machine.

2.2.    Dynamic mathematical model of wheel loader

The diesel engine of the studied machine has a common rail injection system. The most significant part affecting to the engine dynamics is the torque generation in the combustion chamber. This is modelled using a first order system, whose time constant depends on the rotational speed of the engine. The dynamics of fuel injection system is very fast and it is modelled using a 1st order system with a small time constant and a PID-controller. The dynamics of the engine model is verified with separate laboratory measurement data. A detailed description of the engine model is presented in [18] and [19].

The model of the HSD variable displacement pump presents the linear dependency leakage flow and loss torque as a function of port pressures and rotational speed. The equations for the hydraulic pump, and hydraulic fluid volumes are presented in [20] and they are based on [21], [22], [23], [24]. In the simulation model a viscosity of the hydraulic fluid is constant, pressures in the control chambers are distributed evenly

and the pressure of the oil tank is constant. The dynamics of the displacement of the HSD pump are modelled with a delay and a first order transfer function, which is different for increasing and decreasing displacement. The HSD pump displacement controller includes a rate limiter and a cut off pressure functions, which are also modelled. The HSD pump model is verified based on separate step and ramp response measurements. A constant displacement auxiliary hydraulic pump feeding a hydraulic fluid from the tank to the HSD system through the check valves is included to the hydraulic model.

The leakage model of the HSD hub motors with two different configurations for the displacement is formulated the same way as the HSD pump. Mechanical efficiency of the hub motors is modelled with a bristle type dynamic friction torque model presented in [20], based on [25]. Parameters of the HSD motors are based on the measurement data provided by the manufacturer. The dynamics of the displacement change of all the four HSD motors is verified using the measurement data of the field tests instead of laboratory test bench data.

The flushing valve contains one flow control spool and one pressure relief valve after the spool, see Fig 2. Opening of the spool depends of the pressure difference of the A and B port pressures and a certain pressure difference, in this case 16 bar, is needed to open the valve against to the spring. The pressure – volume flow characteristics of the spool is modelled using look-up table data and dynamics of the spool using a first order transfer function. This parameter data was taken from the manufacturer catalogue. All pressure relief valves including one in the flushing valve are modelled with a semi-empirical model using catalogue data of the manufacturer and is described in more detail in [20].

The mathematical model of the mechanics of the studied machine includes models of the machine body and a tyre-road interaction model; see Fig. 3 for schematics of the mechanical model. The tyre-road model is presented in [18], [20]. It is based on [26] and the parameter data was got from the manufacturer. The body of the machine is assumed to be rigid and Matlab/SimMechanics toolbox is used to calculate 6DOF dynamics of the machine. The boom masses were taken from manufacturer data and the axle weights of the machine were measured. Machine body masses and inertia parameters are estimated based on this data.
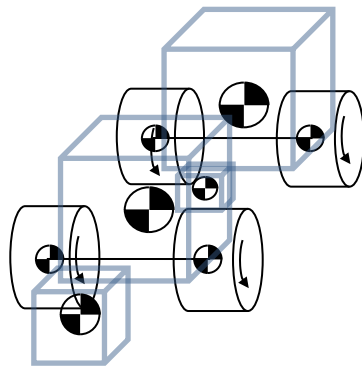


*Figure 3. Schematics of machine mechanical model.*

2.3.   Verification of simulation model

The dynamic mathematical model described in the previous section was verified with the data of over 50 different acceleration/deceleration tests. 13 different tests of these 50 were conducted both with functional flushing valve and without it, and four of them were repeated twice for testing the repeatability. These data were utilized in tuning the parameters of the simulation model. In this paper, three different cases for verification are shown.

The reference signals of the actuators (HSD pump and motor displacements, rotational speed of the diesel engine) of HSD were generated with a computer, but the starting time of acceleration and deceleration phase were defined manually by the user. The measurement data was recorded with 1 kHz sampling frequency to the hard drive of the machine and downloaded after the test to a storage drive. The tests were

done at flat asphalt terrain. Afterwards, the recorded references are used as inputs also to the simulation model. The measured variables for the verification were as shown in Table 1.

*Table 1. Measured variables for verification of dynamic mathematical model.*

| Signal | Range | Unit |
|---|---|---|
| Diesel engine rotational speed | 0…2200 | rpm |
| HSD pump displacement | -100…100 | % |
| Machine velocity | 0…20 | km/h |
| Consumption of diesel engine | 0…20 | kg/h |
| Pressure at port A | 0…400 | bar |
| Pressure at port B | 0…400 | bar |

Figure 4 presents a verification test case 1 in which the machine is accelerated with a predefined 2 s ramp reference change of the HSD pump from 0 to 70% and keeping the diesel rotation speed reference at 1000 rpm. After reaching steady-state the diesel rotation reference was risen stepwise to from 1000 rpm to 1900. Finally, the machine was stopped driving the displacement of the HSD pump to 0 with a 0.7 s ramp. Displacement of the hydraulic motors was held constant (100%) during the test. The temperature of the measured hydraulic fluid was 38 degrees of Celsius in this test case.

In the verification case 2 presented in Fig. 5, the machine was driven with constant diesel engine rotation speed 1300 rpm and rising the displacement of the HSD pump stepwise from 0 to 60%. In the measurement of the pump displacement there can be seen slight overshoot. Because of the first order dynamics of the HSD pump model this phenomenon cannot be seen at the simulation curve. However, this does not give a big error to the operation of the machine, especially because the pump very rarely is controlled with stepwise control signal, and there is no need to use a second order model. At the time 8 s, the hydraulic motors were set to the half displacement and the velocity is increased from about 8 m/s to 15 m/s. In this measurement the temperature of the hydraulic fluid was only 23 degrees of Celsius and because of this the velocity of the machine is about 0.6…0.8 m/s greater than the simulated velocity in the steady state. In all simulations the viscosity of the hydraulic fluid was kept as a constant.

Figure 6 presents a verification test in which the flushing valve is inactive. The machine was accelerated with a predefined 2 s ramp reference change of the HSD pump (from 0 displacement to 50 %) and stopped with a 0.5 s ramp. In this test case, the hydraulic motors were set to half displacement. In this case, the verification results are also satisfactory, as they were also in all other test cases not discussed in this paper. It can be concluded that the model is suitable to be used in anomaly detection and diagnostics study presented in Sections 3 and 4, as well as in control system development presented in [27]. It should be highlighted, that the direct comparison between the measurements with active and inactive flushing valve for fault detection purposes is impossible and some other approach is needed.

Random (short time, high amplitude) error values were detected in some wheel speed measurements, which were done using Hall sensors and a gear ring installed in the wheel axles. Because of this the velocity measurement of the machine was not used at the time series data analysis discussed in Section 4.
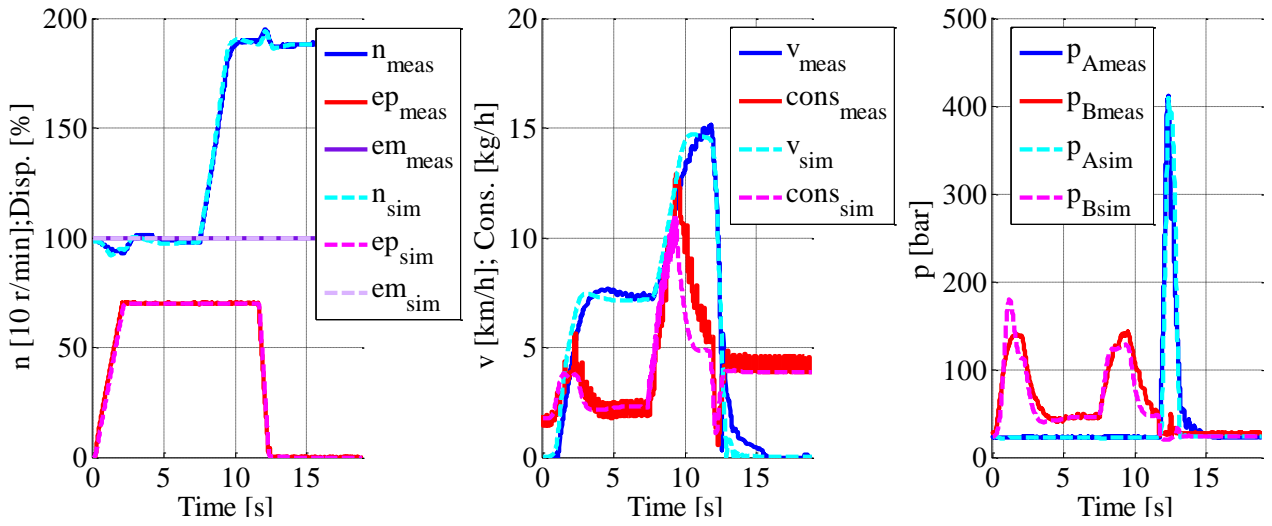
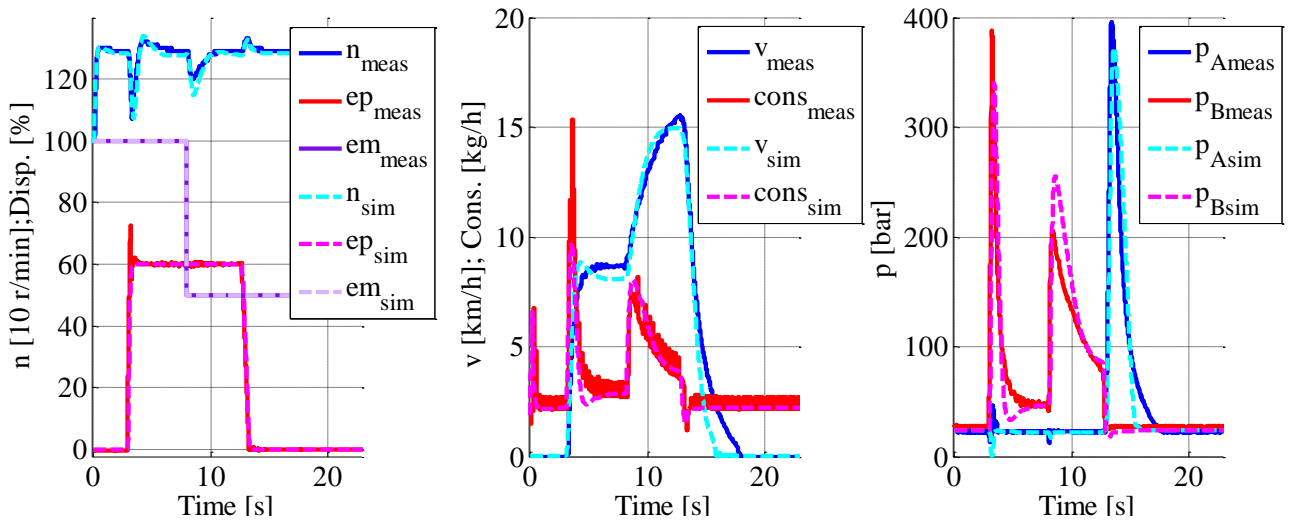*Figure 4. Verification case 1. With flushing valve.*



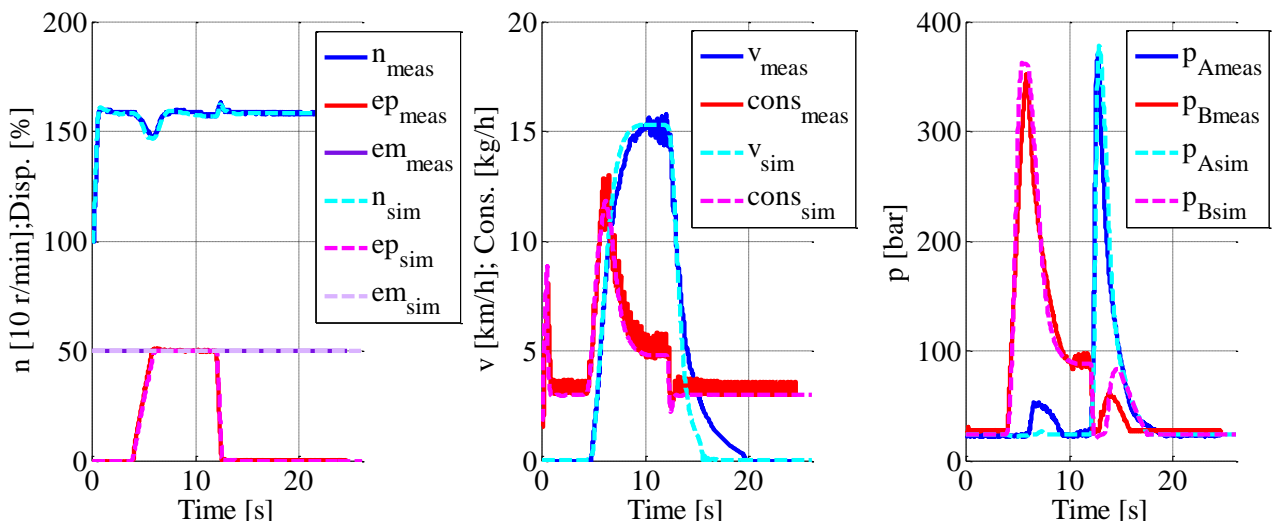*Figure 5. Verification case 2. With flushing valve.*



*Figure 6. Verification case 3. Without flushing valve.*

## 3. ANALYSIS OF TIME SERIES DATA

Analysing and comparing the responses of a real work machine and a corresponding dynamic mathematical model can reveal deteriorated conditions and evolving failures. In this study, a statistical method called a joint probability distribution [16] is utilized for this purpose. In this method, the main idea is to model the behaviour of the system with probability density functions of the correlation coefficients for segmented multivariate time series data using histograms and test how well the future behaviour fits the model. The modelled histograms are then used to derive the joint probability values and furthermore the distributions of these values. Comparison of the joint probability values of multiple variables of individual segments or whole drive sequence enables us to detect effectively different anomalies [16].

When the correlation coefficients of the segmented multivariate data belong to sections of histograms where the probability is very low, then it is treated as rare occasion and the probability of an anomaly is high. Again, if the correlation coefficients belong to sections where the probability is high, it is treated as normal behaviour. On the basis of this information further actions can be targeted on essential subsystems and specific work movements. The main goal is not to try to allocate reasons for possible differences to a specific part of a component or even to a component. The output from the analysis is to verify whether all machine functions correspond to the requirements and to reveal response anomalies and other characteristics in machine operation. The complete procedure for the analysis of time series data will be explained in the following sections.

### 3.1. Data selection and segmentation

In the analysis, the data are first selected and parsed from the measurements to acquire specifically the data from the acceleration and deceleration phases. This way we can reduce the data dimensionality, synchronize and capture the most relevant data in regards to the analysis [9].

After data selection, the data sets are segmented (i.e. divided) into equal lengths where the segments are overlapping. Segmentation allows the dividing of time series data into smaller groups of data sets which describe the patterns of the measured variables. Segmentation enables allocation of the segments in the time series data that generates anomalies. The length of the segments was chosen long enough to capture transient periods which contain the most relevant data in regards to anomaly detection and diagnostics, but not too long, because otherwise the contribution of the important phenomena in the correlation coefficients decreases.

The measured signals after data selection are denoted $x_i$ for $i = 1, ..., m$, where $m$ is the number of signals of interest. We will assume $N$ data segments and let data segment $j$ contain $n$ data samples sampled at time instances $t_1^j, ..., t_n^j$ for $j = 1, ..., N$. Our earlier assumption on overlapping segments thus requires that $t_1^j < t_1^{j+1} < t_n^j$.

### 3.2. Estimated distribution of correlation coefficients and observed joint probability distributions

In different sub-systems of a machine, the data signals are mostly dependent to each other and in case of an anomaly these dependencies change in certain way. We will build statistical models of these dependencies and use these models to discriminate the faulty machines by detecting when the correlations deviate from the model of the undamaged machine.

When two sets of data are strongly linked together they have a high correlation. To compare extracted segments of multiple variables, correlations are calculated for each variable pair. The correlation coefficient, denoted by r, tells how closely data in a scatterplot fall along a straight line. The closer the absolute value of $r$ is to one, the better the data are described by a linear equation. The value $r = 1$ means a perfect positive correlation, and the value $r = -1$ means a perfect negative correlation. Data with values of $r$ close to zero

show little to no straight-line relationship. Pearson's correlation coefficient [28] is defined in Eq. 1. For segment $j$, correlation between $x_i$ and $x_k$ is given by

$$r_{i,k}(j) = \frac{\sum_{p=1}^{n}\left(x_i(t_p^j) - \overline{x}_{i,j}\right)\left(x_k(t_p^j) - \overline{x}_{k,j}\right)}{\sqrt{\sum_{p=1}^{n}\left(x_i(t_p^j) - \overline{x}_{i,j}\right)^2 \sum_{p=1}^{n}\left(x_k(t_p^j) - \overline{x}_{k,j}\right)^2}} \tag{1}$$

where

$$\overline{x}_{i,j} = \frac{1}{n}\sum_{p=1}^{n} x_i(t_p^j) \tag{2}$$

is the mean value of segment $j$ of signal $x_i$. Other correlation coefficients and mean values are defined in similar manner.

The behaviour of an undamaged machine is then modelled by probability density functions of these correlation coefficients using histograms and test how well the future behaviour fits the model. In histogram calculation, interval $[-1,1]$ is divided to $M$ bins. Then, to calculate probability distribution $p_{i,k}$, the number of times that $r_{i,k}(j): j = 1, \ldots, N$ falls in each bin is counted and normalized such that sum of $p_{i,k}$ over all bins equals 1. Logarithmic scale is used to present $p_{i,k}$. Therefore, small positive values are added to zero probabilities before normalization to avoid singularity at zero. Notice that $r_{i,i} = 1$ and that correlation is a symmetric function, that is, $r_{i,k} = r_{k,i}$. Therefore, we will only calculate $p_{i,k}$ for $i, k \in \Pi$, where $\Pi = \{(i,k): i, k = 1, \ldots, m \text{ and } i < k\}$.

After the the statistical models (i.e. probability distributions of correlation coefficients) are built, those can be evaluated using the measured signals of the test machine. This means, for every extracted segment, correlation coefficients $r_{i,k}$ for $i, k \in \Pi$ are calculated as described in the previous section. Now, probability of outcome $r_{ik}$ can be evaluated using $p_{i,k}(r_{i,k})$ function, that is, the value of $p_{i,k}$ at the bin where $r_{i,k}$ falls. Further, we will now calculate how probable this segment is using joint probability of all the correlation coefficients given by

$$P = \sum_{(i,k)\in\Pi} p_{i,k}(r_{i,k}) \tag{3}$$

When most of the correlation coefficients are highly probable, value of $P$ is large, and probability of an anomaly is really low (i.e. anomaly is not detected). Otherwise, when large portion of correlation coefficients have low probabilities, $P$ becomes small and anomaly is detected. Threshold values are used for $P$ under which anomalies are detected.

## 4. EXPERIMENTS AND ANALYSIS RESULTS

Both, the wheel loader and its dynamic mathematical model (i.e. simulation model) were used to generating the analysed data. A jammed flush valve of the hydrostatic transmission was used as a fault case (an anomaly). To a healthy machine we refer as undamaged and to a machine with the fault as damaged. We used the similar type of control inputs to drive the real undamaged and damaged machines, and the dynamic mathematical model to generate comparable time sequences both for statistical modelling and tests.

First, we drove the undamaged machine according the defined test case. The control signals were recorded to be used for the mathematical model. The used test drive case was the following: acceleration (driving straight) – deceleration – stopping. The reference control signals for acceleration and deceleration are predefined for each experiment but starting and stopping the test drive is done manually. All the test drives were carried out without any additional load. We measured 17 sets of data in case undamaged and

simulated machine and seven sets of data in case of damaged machine as shown in Table 2. So altogether 41 test drives were completed. Undamaged and damaged data sets are actually part of the verification measurements which were chosen for analysis: see verification measurements in Section 2.3.

*Table 2. Number of measured test drives and their use in analysis.*

| Machine | Training | Test |
|---|---|---|
| Undamaged | 10 | 7 |
| Simulated | 10 | 7 |
| Damaged | - | 7 |

Four variables were measured in each experiment as shown in Table 3. The sampling frequency was 100 Hz (resampled from verification measurements). 20 test drives from these 41 data sets were used in the training phase (statistical model generation) and 21 in the testing phase of the analysis: see table 2. Although, the driven test drives are quite similar, there are still differences and it was the purpose of our research to show that this methodology works even when the tested data sets are driven with different but still similar type of control inputs than used in the statistical model generation.

*Table 3. Analysed variables of HSD.*

| Signal | | Range | Unit |
|---|---|---|---|
| $s_1$ | Diesel engine rotational speed | 0…2200 | rpm |
| $s_2$ | HSD pump displacement | -100…100 | % |
| $s_3$ | Pressure at port A | 0…400 | bar |
| $s_4$ | Pressure at port B | 0…400 | bar |

Data selection is based on the HSD pump displacement signal. The analysed signals are combined of three parts: 1) $a = 400$ data points after the displacement starts to rise (i.e. is higher than zero), 2) $b = 200$ data points before the displacement decreases to zero and 3) $c = 200$ data points after the displacement reaches zero displacement at the end of the test drive: see Fig. 7. This same procedure is done to all the analysed signals using the information (i.e. specific points a,b and c in time series data) of data selection acquired from the corresponding displacement signal.
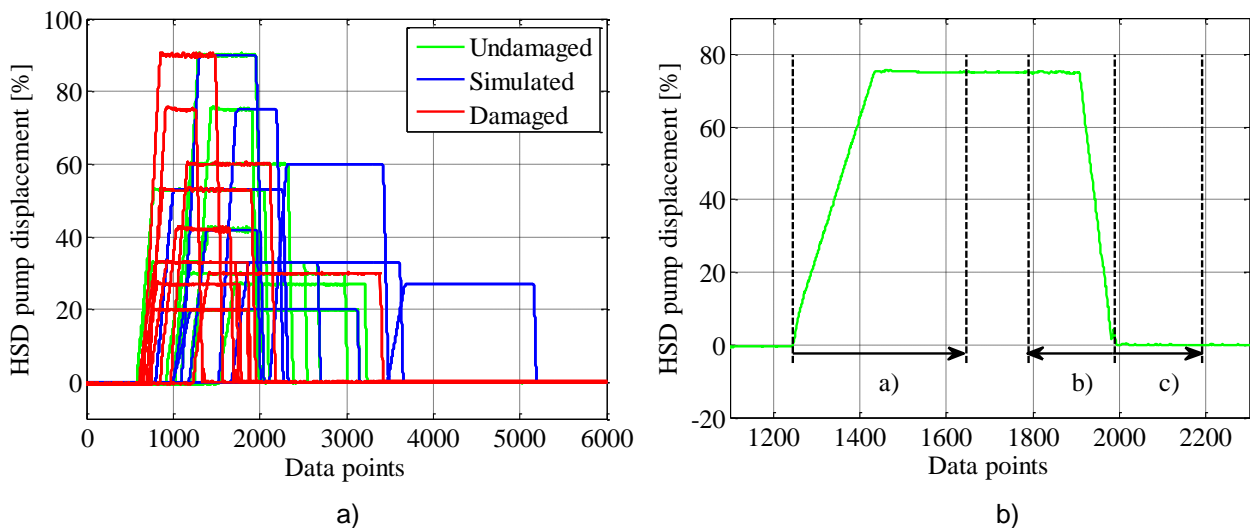


*Figure 7. Data selection based on HSD pump displacement data: a) raw HSD pump displacement data, b) example of data selection.*

Measured variables from all the test drives used in the analysis in the case of undamaged, simulated and damaged machines are shown in Fig. 8. The data shown in Fig. 8 is already selected according the procedure described previously.
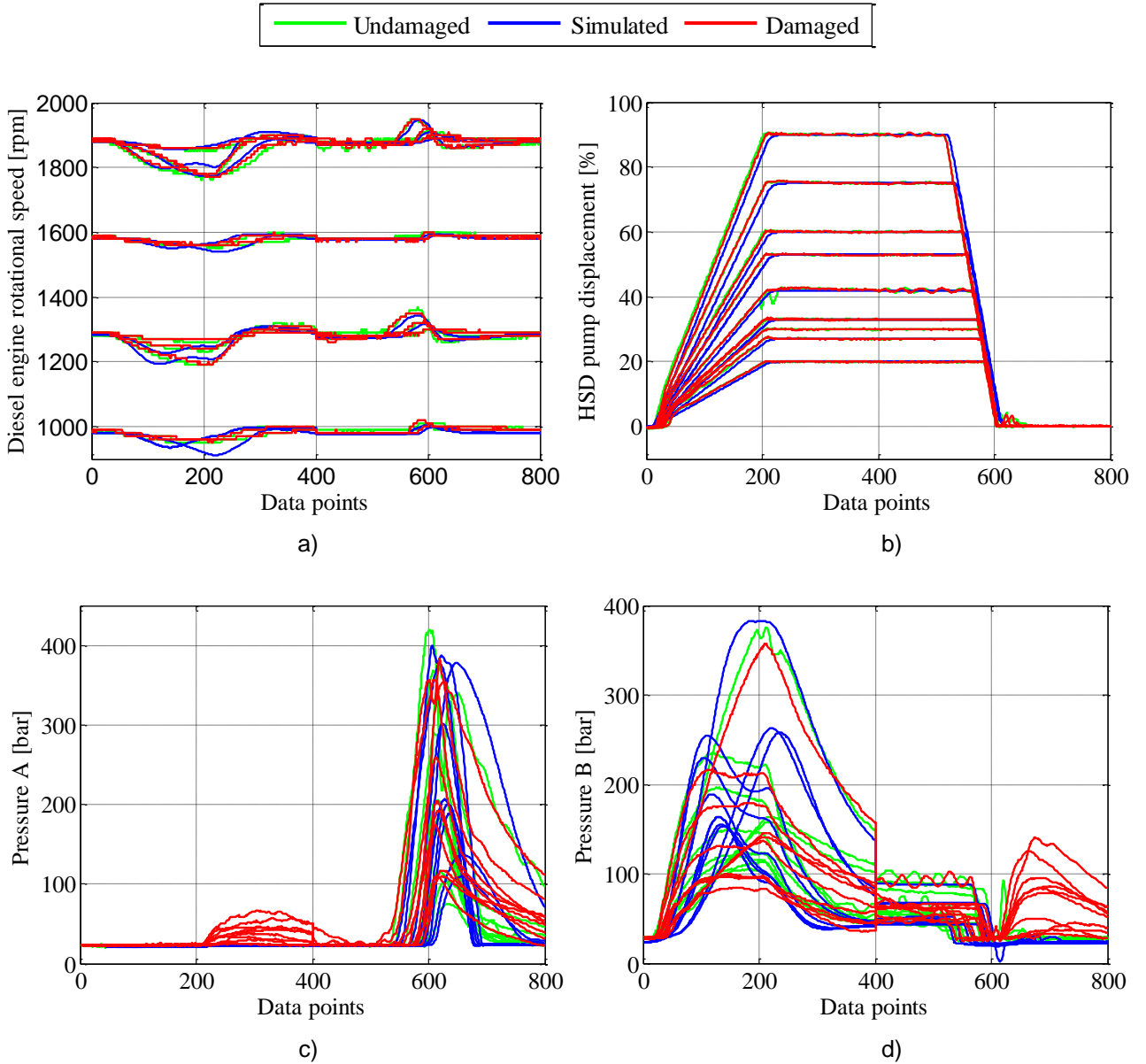
*Figure 8. Analysed data in case of real undamaged, simulated and real damaged machines: a) diesel engine rotational speed, b) HSD pump displacement, c) pressure A and d) pressure B.*

After data selection, each data set contained 800 data points for each measured variable. The measurements were segmented into parts of the same length. The length of the segment was $n = 100$ with 50 overlapping data points. Thus the number of segments equal $N = 15$ for each data set.

In modelling of probability density functions, every extracted segment included $m = 8$ variables, that is, $x_i: i = 1, ..., 8$, where $x_i: i = 1, ..., 4$ are signals $s_i: i = 1, ..., 4$ (defined in Table 3) of the undamaged machine, and $x_i: i = 5, ..., 8$ are signals $s_i: i = 1, ..., 4$ of the mathematical model. This means altogether 28 correlation coefficients. Probability density functions for these correlation coefficients were computed using histograms. The histogram, interval [-1, 1] was divided into $M = 21$ bins.

In testing phase, the correlation coefficients $r_{i,k}$ for $i, k \in \Pi$ are calculated in the same way as in the training using the undamaged or the damaged machine ($x_i: i = 1, ..., 4$) against the mathematical model. The mutual correlations of the simulated machine ($r_{1,2}, r_{1,3}, r_{1,4}, r_{2,3}, r_{2,4}, r_{3,4}$) were omitted. Based on earlier research, those correlation coefficients do not contain information which would help in anomaly detection [16]. Therefore, we used only the remaining 22 correlation coefficients.

After that, we calculate $P$ for each segment to obtain $P_n$ which is the sequence of the joint probabilities $P$ for $n = 1, .., N$. Fig. 9 shows joint probability distributions of training (statistical model generation) and testing

with calculated mean values of the distributions and defined static threshold for anomaly detection. The differences between the undamaged and the damaged machines can be clearly seen.
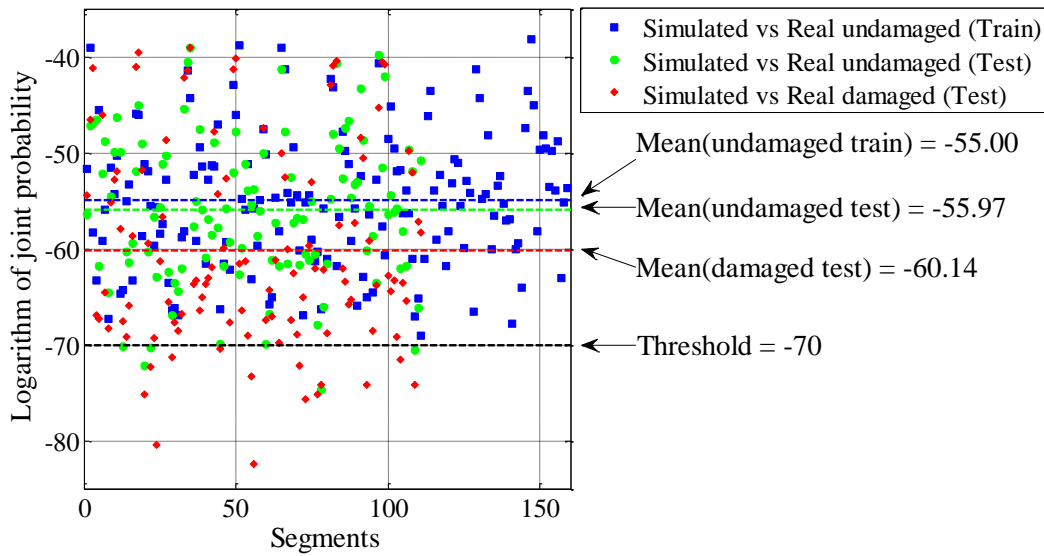


*Figure 9. Joint probability distributions of training and testing data. Static Threshold for anomaly detection and mean values of joint probability distributions are shown.*

The diagnostics is finally based on thresholds. Using a static threshold for every segment, which is a little smaller than the smallest $P$ in the case of the undamaged machine, we can detect the presented fault. So if $P$ in a segment is smaller than the threshold, then this segment is treated as anomaly. This enables also the combining of the anomalies with the operating states of the machine. From Fig. 9 can be seen that there are segments which have very low $P$ value. These segments are very rare or they do not appear at all in the training phase. It indicates a high probability of an anomaly. When the static threshold is defined to be smaller than the smallest value of the statistical model, here -70, we can detect anomalies that have smaller $P$. Because the data sets in the testing were slightly different than in the model generation, it can also be noticed that some of the segments in the testing in the case of the undamaged machine gets a $P$ which is lower than the defined threshold. Therefore, the threshold value could be lowered a little to get rid of this phenomenon. Table 4 shows the number of segments under the static threshold using the value -70.

*Table 4. Anomaly detection using static threshold (i.e. segments under threshold).*

| Undamaged train | Undamaged test | Damaged test |
|---|---|---|
| 0/111 (0 %) | 5/111 (4.5 %) | 14/111 (12.6 %) |

In addition to the static threshold, a threshold based on the arithmetic mean of $P_n$ from one test drive or longer period containing several test drives can be used. In this way, both the single segments with low probability values, which indicate high probability of an anomaly, and also changing trends of the system can be detected. The mean value of the damaged machine is clearly lower than in the case of the undamaged machine, see Fig. 9. In testing, the difference between the mean value of the damaged machine (red) and the mean value of the statistical model of the undamaged machine (blue) is over five times higher (529%) compared to the undamaged machine (green).

## 5. CONCLUSIONS

Anomaly detection and diagnostics of a wheel loader was studied using a real machine (wheel loader), a dynamic mathematical model of this machine and joint probability distributions. The dynamic mathematical model of the wheel loader and its sub-components were verified with several different laboratory and field measurements. The verification results of three different cases were presented in the paper. Based on the

verification results can be concluded that the model is suitable to be used in anomaly detection and diagnostics study.

The HSD of the wheel loader was selected as analysed sub-system of the machine. A jammed flush valve of the hydrostatic transmission was used as an anomaly to study the changes in the joint probability values and to verify the results of the anomaly detection and the diagnostics. Altogether, 41 test drives, 24 with the real machine and 17 with the dynamic mathematical model, were carried out to obtain measurement data for analysis purposes. The measured data comprised of four variables describing the behaviour of the HSD.

Experimental results of anomaly detection and diagnostics were presented using a combination of a static threshold and a threshold based on the arithmetic mean of the joint probability distribution. This enables detection of both single segments with low probability values indicating anomalies and also changing trends of the system. The central point of the joint probability distribution method is that the probabilities of the multiple correlation coefficients of the variable pairs are compared, instead of comparing the responses or even the calculated correlations directly. Combining these probabilities enables the detection of anomalies, rare situations with low probabilities, from which one can conclude there is something wrong in the system or the subsystem. Joint probability distributions were calculated for the test drives using the computed histograms of the correlation coefficients. The experimental results show clearly lower probabilities for test drives where fault is present compared to ones without faults.

The analysing methodology which is used in this study enables the detection of sudden critical faults as well as slowly evolving faults. The simultaneous examination of several variables enables also a more generic approach of detecting several different anomalies and applying it to different machine types.

NOMENCLATURE

| Designation | Denotation | Unit |
|---|---|---|
| $cons_{meas}$ | Measured fuel consumption | [kg/h] |
| $cons_{sim}$ | Simulated fuel consumption | [kg/h] |
| $\bar{e}$ | Arithmetic mean of error | [-] |
| $em_{meas}$ | Measured displacement of hydraulic motor | [%] |
| $em_{sim}$ | Simulated displacement of hydraulic motor | [%] |
| $ep_{meas}$ | Measured displacement of pump | [%] |
| $ep_{sim}$ | Simulated displacement of pump | [%] |
| $k$ | Number of variables | [-] |
| $M$ | Number of bins | [-] |
| $N$ | Number of segments | [-] |
| $m$ | Number of data signals | [-] |
| $n$ | Number of data points | [-] |
| $n_{meas}$ | Measured rotational speed of diesel engine | [rpm] |
| $n_{sim}$ | Simulated rotational speed of diesel engine | [rpm] |
| $P$ | Joint probability value | [-] |
| $p_{A_{meas}}$ | Measured pressure A | [bar] |
| $p_{B_{meas}}$ | Measured pressure B | [bar] |

| | | |
|---|---|---|
| $p_{A_{sim}}$ | Simulated pressure A | [bar] |
| $p_{B_{sim}}$ | Simulated pressure B | [bar] |
| $p_{i,k}(r_{i,k})$ | Probability of $r_{i,k}$ | [-] |
| $P_{min}$ | Minimum joint probability value | [-] |
| $P_n$ | Joint probability distribution | [-] |
| $\bar{P}$ | Mean of joint probability | [-] |
| $r$ | Correlation coefficient | [-] |
| $r_{i,k}(j)$ | Correlation between $x_i$ and $x_k$ for segment $j$ | [-] |
| $s^2$ | Variance | [-] |
| $s_i$ | Analysed signals | [-] |
| $t_1^j, \dots, t_n^j$ | Time instances on which $n$ data samples in data segment $j$ are sampled | [-] |
| $v_{meas}$ | Measured velocity of machine | [km/h] |
| $v_{sim}$ | Simulated velocity of machine | [km/h] |
| $x_i$ | Data vector | [-] |
| $\bar{x}_{i,j}$ | Mean value of segment $j$ of signal $x_i$ | [-] |
| $x_k$ | Data vector | [-] |
| $\bar{x}_{k,j}$ | Mean value of segment $j$ of signal $x_k$ | [-] |
| $\sum e$ | Accumulated error of $P_n$ | [-] |

REFERENCES

[1]     Struss, P., Provan, G., de Kleer, J. and Biswas, G. Special Issue on Model-Based Diagnostics. *IEEE Transactions on systems, Man, and Cybernetics - Part A: Systems and Humans*, 40(5): 870 – 873, 2010.

[2]     Hwang, I., Kim, S., Kim, Y., and Seah, C.E. A Survey of Fault Detection, Isolation, and Reconfiguration Methods. *IEEE Transactions on Control Systems Technology*. 18(3):636-653.

[3]     Miljkovic, D. Fault Detection Methods: A Literature Survey. In: *Proceedings of the 34th International Convention MIPRO 2011*, Opatija, Croatia , May 23-27, 2011, pp. 750-755.

[4]     Kim, H-E. *Machine Prognostics Based on Health State Probability Estimation*. PhD dissertation, Faculty of Built Environmental Engineering, Queensland University of Technology, 2010.

[5]     Dongliang, L. *Estimation of Stochastic Degradation Models Using Uncertain Inspection Data.* PhD dissertation, University of Waterloo, 2012.

[6]     Fuchs, E., Gruber, T., Nitschk, J. and Sick, B. Online Segmentation of time series based on polynomial least-squares approximations. *IEEE Transactions on Pattern Analysis and Machine Intelligence*, 32(12):2232-2245, 2010.

[7]     Keogh E, Chu S, Hart D and Pazzani M. An Online Algorithm for Segmenting Time Series. In: *Proceedings of IEEE International Conference on Data Mining*, San Jose, CA, USA, 29 November – 02 December,  2001, pp. 289-296.

[8]     Khalid, S., Khalil, T. and Nasreen, S. A survey of feature selection and feature extraction techniques in machine learning. In: *Proceedings of Science and Information Conference* 2014, London, UK, 27-29 August, 2014, pp. 372-378.

[9]     Krogerus, T. *Feature Extraction and Self-Organizing Maps in Condition Monitoring of Hydraulic Systems*. PhD thesis, Department of Intelligent Hydraulics and Automation, Tampere University of Technology, 2011. (available: http://URN.fi/URN:NBN:fi:tty-2011081914759)

[10]     Zhang, Z., Shao, X. and Yu, D. Fault Diagnosis of a wheel Loader by Artificial Neural Networks and Fuzzy Logic. In: *Proceedings of 2006 IEEE Conference on Robotics, Automation and Mechatronics*, Bangkok, Thailand, 7 - 9 June, 2006, pp. 1-5.

[11]     Aly, M. *Survey on Multi-Class Classification Methods*. Technical Report, Caltech, USA, 2005.

[12]     Prabhu, S. Model-Based Design for Off-Highway Machine Systems Development. *SAE Technical paper 2007-01-4248*, 2007.

[13]     Moghaddam, R. and Lipsett, M. Modeling, simulation & fault detection in excavators with time-varying loading. In: *Proceedings of 2010 IEEE/ASME International Conference on Advanced Intelligent Mechatronics*, Montreal, ON, USA, 6-9 July, 2010, pp. 779 - 784.

[14]     Multanen, P. and Hyvönen, M. Utilization of R&D simulators to support the maintenance of mobile work machines. In: *Proceedings of the eighth international conference on condition monitoring and machinery failure prevention technologies*, Cardiff, UK, 20-22 June, 2011, pp. 1-12.

[15]     Hietala, J-P., Krogerus, T., Multanen, P., Hyvönen, M. and Huhtala, K. Novel Procedure for Supporting Maintenance of Mobile Work Machines Using R&D Simulators. In: *Proceedings of the Eleventh International Conference on Condition Monitoring and Machinery Failure Prevention Technologies*, CM 2014 and MFPT 2014, Manchester, UK, 10-12 June 2014, pp.1-9.

[16]     Krogerus, T., Hyvönen, M., Multanen, P., Hietala, J-P. and Huhtala, K. Joint Probability Distributions in the Diagnostics of Mobile Work Machines, *Mechatronics*, *The Science of Intelligent Machines*, 2014. (in review)

 [17]     Backas, J., Ahopelto, M., Huova, M., Vuohijoki, A., Karhu, O., Ghabcheloo, R. and Huhtala, K. 2011. IHA-Machine: A Future Mobile Machine. In: *Proceedings of The Twelfth Scandinavian International Conference on Fluid Power*, *SICFP'11*, Tampere, Finland, May 18-20, 2011, Vol. 4, pp. 161-176. (available: http://URN.fi/URN:ISBN:978-952-15-3273-3)

[18]     Erkkilä, M., 2007, Dynamic Model of CVT Power Train, In: *Proceedings of the Tenth Scandinavian International Conference on Fluid Power*, Tampere, Finland, May 21-23, 2007.

[19]     Tsal, S. and Goyal M. Dynamic Turbocharged Diesel Engine Model for Control Analysis and Design, *SAE Technical Paper 860455*, 1986.

[20]     Hyvönen, M., Vilenius, J., Vuohijoki, A. and Huhtala, K. Mathematical Model of the Valve Controlled Skid Steered Mobile Machine. In: *Proceedings of 2$^{nd}$ International Conference on Computational Methods in Fluid Power*,  Aalborg, Denmark, August 2-3,  2006.

[21]     Ivantysyn, J. and Ivantysynova, M. Hydrostatic pumps and motors: Principles, Design, Performance, Modelling, Analysis, Control and Testing. New Delhi: Akademia Books Int., 2001.

[22]     Huhtala, K. *Modeling of Hydrostatic Transmission Steady State, Linear and Non-linear Models*. PhD thesis, Institute of Hydraulics and Automation, Tampere University of Technology, 1996.

[23]     Merritt, H. *Hydraulic Control Systems*, New York: J. Wiley & Sons Inc., 1967.

[24]     Canudas de Wit, C., Olsson, H., Åström, K. and Lischinsky, P. A New Model for Control Systems with Friction. *IEEE Transactions on Automatic Control*, 40(3):419-425, 1995.

[25]     Pacejka, H. *Tyre and vehicle dynamics*, Oxford: Butterworth-Heinemann; 2002.

[26]     McCloy D and Martin HR. The Control of Fluid Power. London: Longman Group Limited; 1973.

[27]     Backas, J., Ghabcheloo, R., Hyvönen, M. and Huhtala, K. Fuel Optimal Controlled for Hydrostatic Drives - A Simulation Study and Model Validation. In: *Proceedings of the ASME/BATH 2014 Symposium on Fluid Power & Motion Control, FPMC2014*, Bath, UK, September 10-12, 2014, pp. 1-11.

[28]     Gibbons, J.D. *Nonparametric Statistical Inference*, New York: Marcel Dekker Inc.; 2003.